



1 Extreme storms during the last 6,500 years from lagoonal  
2 sedimentary archives in Mar Menor (SE SPAIN)

3  
4  
5

6 Dezileau L. <sup>\*</sup>,<sup>1</sup>, Pérez-Ruzafa A. <sup>2</sup>, Blanchemanche P. <sup>3</sup>, Degeai J.P. <sup>3</sup>, Raji O. <sup>1,4</sup>,  
7 Martinez P. <sup>5</sup>, Marcos C. <sup>2</sup> and Von Grafenstein U. <sup>6</sup>

8  
9

10 [1]{Université de Montpellier, Geosciences Montpellier, CNRS, UMR 5243}

11 [2]{Universidad de Murcia, Departamento de Ecología e Hidrología, Regional Campus of International Excellence  
12 Campus Mare Nostrum, Murcia 30100, Spain}

13 [3]{Université Montpellier 3, Laboratoire d'Archéologie des Sociétés Méditerranéennes, CNRS, UMR 5140}

14 [4]{Department of Earth Sciences, Université MohammedV-Agdal, Rabat, Morocco}

15 [5]{Université Bordeaux 1, EPOC, CNRS, UMR 5805}

16 [6]{Laboratoire des Sciences du Climat et de l'Environnement, CNRS/CEA, Saclay}

17  
18

19 \* Correspondence to : laurent.dezileau@gm.univ-montp2.fr

20



21

## 22 Abstract

23 Amongst the most devastating marine catastrophes that can occur in coastal areas, are storms and  
24 tsunamis, which may seriously endanger human society. Many such events are known and have  
25 been reported for the Mediterranean, a region where high-frequency occurrences of these extreme  
26 events coincides with some of the most densely populated coastal areas in the world. In a  
27 sediment core from Mar Menor Lagoon (SE Spain), we discovered eight coarse grained layers  
28 which document marine incursions during periods of intense storm activity or tsunami events.  
29 Based on radiocarbon dating, these extreme events occurred around 5250, 4000, 3600, 3010,  
30 2300, 1350, 650 and 80 years cal B.P.. No comparable events have been observed during the 20<sup>th</sup>  
31 and 21<sup>th</sup> centuries. The results indicate little likelihood of a tsunami origin for these coarse grained  
32 layers, although historical tsunami events are recorded in this region. These periods of surge  
33 events seem to coincide with the coldest periods in Europe during the late Holocene, suggesting a  
34 control by a climatic mechanism for periods of increased storm activity. Spectral analyses  
35 performed on the sand % revealed four major periodicities of  $1228 \pm 327$ ,  $732 \pm 80$ ,  $562 \pm 58$ , and  
36  $319 \pm 16$  yr. Amongst the well-known proxies that have revealed a millennial-scale climate  
37 variability during the Holocene, the ice-rafted debris (IRD) indices in North Atlantic developed  
38 by Bond et al. (1997, 2001) present a cyclicity of  $1470 \pm 500$  yr, which matches the  $1228 \pm 327$  yr  
39 periodicity evidenced in the Mar Menor lagoon, considering the respective uncertainties on the  
40 periodicities. Thus, an in-phase storm activity in Western Mediterranean is found with the coldest  
41 periods in Europe and to the North Atlantic thermohaline circulation. However, further  
42 investigations, such as additional coring, high-resolution coastal imagery, are needed to better



43 constrain the main cause of these multiple-events.

44

45

46

47 Keywords: coastal lagoons, storm, tsunami, Mediterranean Sea, Late Holocene.

48

49

## 50 1. Introduction

51 In the last century the Mediterranean coastal zones have undergone a considerable development  
52 and the coastal hazards incidence has significantly increased. The coastal zones are exposed to  
53 flooding and coastal erosion processes, and are highly vulnerable to extreme events, such as  
54 storms, cyclones or tsunamis, that can cause significant losses (Seisdedos et al., 2013).

55 Mediterranean intense storms and cyclones are rare meteorological phenomena observed in the  
56 Mediterranean Sea. Different climatological and meteorological works in the western  
57 Mediterranean area show that extreme storms and cyclones show a complex variability in the  
58 sense of non-uniform spatial and temporal patterns (Trigo et al., 2000; Lionello et al., 2006;  
59 Gaertner et al., 2007). This is in partly due to the lack of a clear large scale pattern which may be  
60 expeted when dealing with intense events, as the number of events is low with irregular intensity  
61 and intervals. More long-term observations or paleo-reconstructions in different area of the  
62 western Mediterranea are needed. Tsunamis are known to occur in the Mediterranean Sea where  
63 all types of sources-earthquakes, volcanic eruptions and landslides from the continental margins  
64 are active. There are evidences of intense tsunamis during the historical and pre-historical period,  
65 especially in the tectonically more active eastern Mediterranean (e.g., Kelletat and Schellmann,



66 2002 ; Morhange et al., 2006). The western part of the basin has also been reported as tsunami-  
67 exposed. Historic events have been reported from the Algerian coast and tsunami propagation has  
68 been modelled (Alvarez-Gomez et al., 2011). Geomorphic evidence of ancient tsunami impacts  
69 has also been documented (Maouche et al., 2009). A long-term record of tsunami and storm  
70 activity on time scales of centuries to millennia is especially important in understanding the  
71 temporal variability of these extreme events.

72

73 This study focuses mainly on the Murcia province in Spain (Figure 1). This  
74 Mediterranean coast is sensitive for the risks of submersion during extreme events. We propose  
75 to use a high-resolution geochemical and sedimentological approach to reconstruct past surge  
76 events in the Mar Menor lagoon, and then confront our results with extreme historical coastal  
77 events in the western Mediterranean.

78

## 79 2. Study site

80

81 The Mar Menor lagoon is the largest lagoon of the Spanish Mediterranean coast, located at the  
82 SE of the Iberian Peninsula, in the region of Murcia in the area called Campo de Cartagena basin  
83 (Lat. 37.786129, Lon. 0.810450, Figure 1). This coastal lagoon occupies an area of  
84 approximately 135 km<sup>2</sup> with an average depth of 3.6 m. This lagoon is separated from the  
85 Mediterranean sea by La Manga, which is a sandy barrier of 20 km long, between 30 and 500 m  
86 wide and less than 3 m above sea level. This sandy barrier is crossed by five, more or less  
87 functional, channels or “golas”. The Campo de Cartagena Basin represent 1,440 km<sup>2</sup>, with an  
88 elevations ranging from the sea level to 1065 m, surrounded by the Mediterranean sea to the East,



89 the anticline of Torrevieja to the North and the Cartagena-La Unión mountain range to the south.  
90 This basin is filled by sediments from early Miocene to quaternary. The major lithologies are  
91 sand, silt, clay conglomerate, caliche and sandstone (Quaternary); marl, conglomerate and  
92 gypsum (Miocene, Pliocene) (Jiménez-Martinez et al, 2012). The lagoon and the northern salt  
93 marshes of San Pedro are protected for their ecological importance (Special Protected Area of  
94 Mediterranean Interest, Natura 2000 network and Ramsar). The area is impacted by residual past  
95 mining activity, agricultural activities (intensive fruits and vegetable production), and urban  
96 growth coupled with touristic development since 1956 (Pérez-Ruzafa et al., 1987; 1991; 2005).  
97 Most of La Manga area is urbanized, a population of 10,000 inhabitants live here all year long,  
98 and growing to ~ 200,000 habitants during summer. High population density and low level  
99 topography makes the area very sensitive to the impact of climate change and sea level rise. Mar  
100 Menor lagoon is considered as one of the Spanish coast most threatened site by the mean sea  
101 level rise and possible increase of extreme climatic events.

102

103

### 104 3. Materials and methods

105

#### 106 3.1 Core material

107

108 A 4-m-long piston core (MM2) was collected in the Mar Menor lagoon in September 2011  
109 (Figure 1) with the UWITEC<sup>®</sup> gravity coring platform (Laboratoire des Sciences du Climat et de  
110 l'Environnement and University of Chambéry) using a simplified piston corer of 2 m length and  
111 83 mm inner diameter. Two consecutive sections (0m to 2 m and 2m to 4m sediment depth,



112 respectively, were cored from a first position followed by a third section (1m to 3m) from a  
113 position ca. 1 m apart to cover the technical hiatus between the first two sections. MM2 core was  
114 collected at 4 m below sea level.

115

### 116 3.2 Physical measures

117

118 Back to the laboratory, the structure of the sediment was studied using the Scopix X-ray scanning  
119 (EPOC, University of Bordeaux 1) and photographed. This was complemented by granulometric  
120 analyses on contiguous 1-cm samples using a Beckman-Coulter LS13320 laser diffraction  
121 particle-size analyser (Géosciences Montpellier). XRF analysis were performed on the surface of  
122 split sediment core MM2 every 0.5 cm using a non-destructive Avaatech core-scanners (EPOC,  
123 Université Bordeaux 1). The split core was covered with a 4  $\mu\text{m}$  thin Ultralene to avoid  
124 contamination. Geochemical data was obtained at different tube voltage, 10 kV for Al, Si, S, Cl,  
125 K, Ca, Ti, Mn, Fe and 30 kV for Zn, Br, Sr, Rb, Zr (Richter et al., 2006).

126

127

### 128 3.3 Macro-fauna

129

130 To study mollusc shells, samples were taken every 2 cm and sieved at 1mm. Individuals were  
131 determined to the lower taxonomic level possible (species or genera) and counted. Assemblage  
132 structure was estimated by mean of species richness (S), taxon abundance ( $n_i$ ) and total  
133 abundance (N).

134



135 3.4 Geochronology

136

137 The chronology of core MM2 was carried out using  $^{137}\text{Cs}$  and  $^{210}\text{Pb}$  method on a centennial time-  
138 scale by gamma spectrometry at the Géosciences Montpellier Laboratory (Montpellier, France).  
139  $^{14}\text{C}$  analyses were realized on mollusk shells at the Laboratoire de Mesure on ARTEMIS in CEA  
140 institute at Saclay. These measurements were obtained from monospecific samples of  
141 *Cerastoderma glaucum* at each level.  $^{14}\text{C}$  ages were corrected for reservoir age (see Sabatier et  
142 al., 2010 for method) and converted to calendar years using the computer program OxCal v4.2  
143 (Bronk Ramsey, 2001, 2008) at two standard deviations (see chapter 4.3).

144

145 3.5 Spectral analyses

146 Cyclic patterns in the Mar Menor lagoonal sequence were studied from spectral analyses by using  
147 several methods in order to reduce possible biases of a single method (Desprat et al., 2003). We  
148 used the maximum entropy method (MEM) and the multi-taper method (MTM). The MEM  
149 selects the spectrum with the highest entropy, which represents the least biased estimate for the  
150 given information, or put in other terms, the maximally noncommittal with regard to missing  
151 information (Harremoës and Topsoe, 2001). The spectrum obtained by this method shows an  
152 excellent frequency resolution with sharp spectral features (Berger et al., 1991; Dubar, 2006;  
153 Pardo-Iguzquiza and Rodriguez-Tovar, 2006). The MTM is a non-parametric method that (1)  
154 reduces the variance of spectral estimates by combining multiple orthogonal windows in the time  
155 domain before Fourier transforming, and (2) provides a narrowband F-test useful to assess the  
156 significance of periodic components (Thomson, 1982, 1990; Percival and Walden, 1993).

157



158

## 159 4. Results

160

### 161 4.1 Core description

162

163 Photo, X-ray images, X-ray fluorescence and high-resolution grain-size analysis for MM2

164 indicate several thin, coarse-grained layers preserved within mud sediments. These coarse layers

165 are constituted by a mixture of shell debris and siliciclastic sand and have basal boundaries easily

166 identified from a change to coarser grain size and darker color on X-ray images (Figure 2).

167 These coarser grain size layers indicate “energetic” events, relative to the background

168 sedimentation (i.e mud facies) and are probably link to washover events (storm or tsunami).

169

### 170 4.2 Sediment source

171 The terrigenous fraction in Mar Menor lagoon is mainly controlled by terrestrial and marine

172 inputs. The core (MM2) was collected at 800 m from the sandy barrier and more than 8,500 m

173 from the different river mouths. On our study site, watercourses are the source of fine fraction

174 dispersed in the lagoon and marine inputs are characterized by coarse sands. The lagoon barrier

175 beach sand samples show unimodal distribution with a mean grain population ranging between

176 160 and 653  $\mu\text{m}$ . The percentages of this grain population decrease from the sea to the lagoon in

177 surface samples. The evolution with depth of this population displays eight main changes in

178 MM2 core revealed by the grey bands on Figure 3. The main peaks of coarse sands occur around

179 5, 40, 60, 150, 170, 210, 255 and 290 cm (Figure 3).



180 Major chemical elements using the ITRAX core scanner provide high-resolution  
181 palaeoenvironmental information in a variety of sedimentary environments. In the present study  
182 we chose the ratio Si/Al and Zr/Al that better discriminate between the two source areas, marine  
183 vs drainage basin (Dezileau et al., 2011, Sabatier et al., 2012; Raji et al., 2015). The high Zr/Al  
184 ratio value is probably explained by the presence of heavy minerals (like zircon) from marine  
185 sand and the high Si/Al ratio is due to Quartz minerals in marine sand. Si/Al and Zr/Al ratios  
186 have the same evolution with depth, especially in the first three meters of the sediment core  
187 (Figure 4, shaded bands).

188 A fundamental step in the core analysis is to establish criteria to correctly identify overwash  
189 layers. We systematically used grain size variation and geochemical signatures (i.e. Si/Al and  
190 Zr/Al ratios). As the background sedimentation shows a fine silt facies, we consider values higher  
191 than 20% of the 63 $\mu$ m fraction as outlining “high energy” events (figure 3). Positive anomalies of  
192 the Si/Al and Zr/Al ratios above 12 and 2,5 respectively (Figure 4), indicate a higher relative  
193 contribution of marine sand. The marine origin of these “high energy” events was also  
194 highlighting through molluscs identification (*Bittium reticulatum* and *Rissoa ventricosa*) (see  
195 chapter 4.3, Figure 6).

196

#### 197 4.3. Faunal variations

198

199 Macro-fauna analyses are a good indicator of a lagoon paleo-isolation state because species  
200 develop in different ranges of salinity, temperature and oxygenation and colonization of marine  
201 species into the lagoon environments depends of the isolation degree and connectivity between



202 both systems. Taxon richness range between 0, at depths higher than 365 cm, and 18 reached at a  
203 260 cm depth

204 The impoverished depths, after the earlier azoic one, corresponds to 302-362 cm with a mean of  
205 4.76 taxons, 72-78 cm with a mean of 5 taxons and 30-36 cm with a mean of 5.7 taxons. The  
206 depths with highest species richness are from 192 to 266 cm and from 81 to 186 cm. These  
207 depths would correspond to a higher marine influence. Above 150 cm take place a progressive  
208 impoverishment in the number of species reflecting a progressive isolation of the Mar Menor  
209 from the Mediterranean, with punctual picks in species richness, probably related to episodes of  
210 rupture of the sandbar (figure 5).

211 The most frequent species, present in more than 50% of the samples, excluding the azoic depths,  
212 are *Corbula gibba* (Olivi, 1792) (92.4%), *Bittium reticulatum* (da Costa, 1778) (84.9%), *Tellina*  
213 sp (78.9%), *Pusillina* (=Rissoa) *lineolata* (Michaud, 1830) (78.2%), *Acanthocardia*  
214 *paucicostata* (G. B. Sowerby II, 1834) (77.3%), *Cerastoderma glaucum* (Bruguière, 1789)  
215 (71.4%), *Anthalis* sp (63.9%), *Abra* sp (74.8%), *Loripes lacteus* (Linnaeus, 1758) (61.3%) and  
216 *Philine aperta* (Linnaeus, 1767) (59.7%). Hydrobiidae sp appear in the 47.9 % of the samples,  
217 but is restricted to the upper 150 cm, constituting the 61.5% of the assemblage at 15 cm depth  
218 section. This specie is a typical lagoon inhabitant. By its part, *Conus ventricosus* (Gmelin, 1791)  
219 appear only in the 13.5% of the samples, comprised between 162 and 293 cm depth, reaching  
220 dominance up to 7% of the assemblage, but characterize typical marine conditions, reinforced  
221 with the presence of abundant seurchin spines.

222 Data of Figure 6 show a main change in mollusc population at around 150-130 cm characterized  
223 by an increase of the most typical lagoonal specie *Hydrobia acuta*, whereas the abundance of  
224 species with marine affinity like *Pusillina* (=Rissoa) *lineolata* and *Conus ventricosus* decrease



225 (Figure 6). This main change in mollusc population also reveals a major palaeoenvironmental  
226 change around 150 cm, this faunal variation is probably due to a change in environmental context  
227 from a lagoonal environment, with a marine influence to a more isolated environment.

228

#### 229 4.3 Age model

230

231 The chronology of core MM2 has been established for the last 6,500 years BP using  $^{137}\text{Cs}$ ,  $^{210}\text{Pb}$   
232 and (AMS)  $^{14}\text{C}$  dates on monospecific shell sample, geochemical analysis of mining-  
233 contaminated lagoonal sediments and paleomagnetism (Dezileau et al., in prep). Radiocarbon age  
234 of lagoonal and marine organisms is usually older than the atmospheric  $^{14}\text{C}$  age and has to be  
235 corrected by subtraction of the “reservoir age” (Siani et al., 2001; Reimer and McCormac 2002;  
236 Zoppi et al., 2001; Sabatier et al., 2010; Dezileau et al., 2015). We evaluated the modern  
237 reservoir  $^{14}\text{C}$  age by comparing an age derived from  $^{137}\text{Cs}$ ,  $^{210}\text{Pb}$  data and geochemical analysis of  
238 mining-contaminated lagoonal sediments with an AMS  $^{14}\text{C}$  age of a pre-bomb mollusc shell (see  
239 Sabatier et al., 2010 for method). The reservoir age (R(t)) with a value of  $1003 \pm 62$   $^{14}\text{C}$  yr is 600  
240 yr higher than the mean marine reservoir age (around 400 yr) and may be explained by an  
241 isolation of the lagoon from the Mediterranean Sea. This high reservoir age value is similar to  
242 other estimates in different Mediterranean lagoons (Zoppi et al., 2001; Sabatier et al., 2010).

243  $^{14}\text{C}$  ages were also obtained on a series of Holocene mollusc shells sampled at different depths of  
244 the ~2-m-long core MM2 (Figure 7, Dezileau et al., in prep). Comparing paleomagnetic ages and  
245  $^{14}\text{C}$  ages versus depth, we show that the reservoir age has changed in the past and was lower (505  
246 yr) than the modern value (1003 yr, Dezileau et al., in prep). This change was also observed in  
247 another Mediterranean lagoons (Sabatier et al., 2010). In the Mar Menor lagoon, Linear



248 Sedimentation Rate (LSR) obtained for the core MM2 suggest a low mean accumulation rate of  
249 0.6 mm.yr<sup>-1</sup>, from the base to the top of the core.

250

## 251 5. Discussion

252

### 253 5.1 Site sensitivity to overwash deposits

254

255 Site sensitivity to overwash deposits may result from different factors such as barrier-elevation,  
256 sediment supply, inlet, and change in sea level (Donnelly and Webb, 2004; Scileppi and  
257 Donnelly, 2007, Dezileau et al., 2011). An increase of sea level induces a shift of the barrier  
258 landward. Therefore, an increase of sand layers in a sediment core may be due to a sea level  
259 change. In the Mediterranean Sea, the sea level has remained more or less constant during the last  
260 5000 yrs (< 2m, Pirazzoli, 1991; Lanbeck and Bard, 2000). Before this period, a significant  
261 change in sea level occurred. During the first phase of lagoonal sediment deposit (between 6500  
262 and 5000 years Cal B.P), the number of sand layers is low. The sandy barrier was probably at  
263 more than 1 km from the present position and may probably explain why sand layers are not  
264 observed. The strong increase in coarse grain layer frequency after ca. 5400 years Cal B.P can be  
265 explained by a migration of the barrier up to a position, which is not far away from the present  
266 position.

267 Fauna content reveals a major palaeoenvironmental change around 150 cm (i.e. 2400 yr cal B.P.,  
268 Figure 6). Such change is probably due to a shift from a leaky lagoon to a restricted and choked  
269 lagoon environment, sensu Kjerfve (1996). Thus, after this date (i.e 2400 yr cal B.P.) the barrier



270 was continuous with sometimes inlet formation in relation to intense overwash events. To  
271 conclude, between 2400 yr cal B.P. and today, the lagoon is isolated from the sea. During this  
272 period the general morphology of the lagoon and the barrier have not changed drastically.  
273 Between 5400 yr cal B.P. and 2400 yr cal B.P. the lagoon was less isolated from the  
274 Mediterranean Sea, typical from a leaky lagoon environment. During this period, fine sediments  
275 were accumulated. The lagoon experienced quiescent sedimentation probably protected behind a  
276 sandy barrier more or less continuous. The presence of sand layers may be interpreted by intense  
277 overwash events. Between 6500-5400 yrs BP, the morphology of the lagoon and the barrier is  
278 different. The position of the sandy barrier was far away from the present position. In that case,  
279 the number and the intensity of surge events recorded are not comparable to the upper part of the  
280 core (Figures 3 and 8). During this period, the lack of sand layers does not mean any surge events  
281 but simply they are not recorded.

282

## 283 5. 2 Storms or tsunamis?

284 The Zr/Al and Si/Al ratios of sandy layers are above 12 and 2,5 respectively (Figure 8),  
285 indicating a higher relative contribution of marine sand. The marine origin of these “high energy”  
286 events was also highlighting through molluscs identification (*Bittium reticulatum* and *Rissoa*  
287 *ventricosa*, Figure 8). This multiproxy approach suggests the occurrence of eight period of  
288 increase of overwash events reflecting perturbations of coastal hydrodynamic due to paleostorm  
289 or paleotsunami events (grey band on Figure 8).

290 Both tsunamis and storms induce coastal flooding. It is difficult to discriminate storm and  
291 tsunami deposits (Kortekaas and Dawson, 2007; Morton et al., 2007; Engel and Brückner, 2011).  
292 The coarse-grained layers observed in the core MM2 could be a signature of tsunamis or storms.



293 Records of historic and contemporary coastal hazards (storms and tsunamis) may help us to  
294 determine which historical events left a sedimentological signature in the Mar Menor lagoon.  
295 In textual archives, extreme storm events were described due to the strong economic and societal  
296 impact of these events (Seisdedos et al., 2013). For the last 200 years, 27 storms affected the  
297 coast of Murcia. Among all of these storms, some seems to be more catastrophic. The storm of  
298 November first, 1869 produced the wreckage of a numerous ships in the Torrevieja harbour.  
299 Between Isla Grosa and San Pedro del Pinatar more than thirty-five ships were collapsed and  
300 crashed. In the Mar Menor lagoon, fifty fishing boats were destroyed and thrown to the ground.  
301 Wave heights associated with this storm were estimated higher than 8 m. This severe storm also  
302 affected La Union and Cartagena cities destroying houses and paralyzing its for many days. From  
303 the hydrological and ecological point of view, the 1869 storm led to drastic and persistent  
304 changes in the salinity of the lagoon and to the colonization of new species of marine origin  
305 (Navarro, 1927), affecting also the fisheries in the lagoon (Pérez-Ruzafa et al., 1991). There are  
306 historical references to some other storms that led to the breaking of the sandbar in the Mar  
307 Menor (in 1526, 1676, 1687, 1690, 1692, 1694, 1706, 1762, 1765, 1787, 1795) (Jiménez de  
308 Gregorio, 1957; Pérez-Ruzafa et al., 1987), although there is no information about their  
309 magnitude, the extent and exact location of the breaks and their impact on the lagoon  
310 environment. Some ups and downs in the number of species observed in Figure 5 could be  
311 related to these events, but an extensive and detailed study would be required for understanding  
312 the relationship between the frequency, duration and intensity of the storms and the spatial and  
313 temporal scales of their effects and their impact on the fossil record.  
314 Different tsunamis occurred on the Spanish coasts, they are more catastrophic and intense on the  
315 Atlantic than on the Mediterranean side (Alvarez-Gomez et al., 2011). In the occidental part of



316 the Mediterranean area, there are historical disastrous tsunami events recorded. In Northern  
317 Algeria, in addition to the 2003 tsunami, the first well documented event remains the tsunami in  
318 the Djijelli Area associated with the seismic event of August 1856, which was also recorded in  
319 the Balearic Islands (Maouche et al., 2009). In the Alboran Sea area some reports mention  
320 tsunamis that affected the African and Spanish coasts in 1790, 1804 and 1522 (IGN, 2009). For  
321 an earthquake magnitude 6.8 (2003 Boumerdes earthquake) with its epicenter calculated at 15 km  
322 offshore of Zemmouri, Wang and Liu (2005) show a regional character of the tsunami  
323 phenomenon from a numerical simulation. The tsunami propagating from the Algerian coast to  
324 the Murcia Province has a lesser amplitude and the tsunami wave height is very low (< 25 cm).  
325 The Boumerdes-Zemmouri tsunami did not induce any damage along the province of Murcia and  
326 the La Manga sandbar. Alvarez-Gomez et al. (2011) identified the hazardous sources and the  
327 areas where the impact of tsunamis is greater from numerical simulations. From a set of 22  
328 seismic tsunamigenic sources, the Maximum Wave Elevation was estimated between 0,5 and 1 m  
329 along the South-Eastern Spanish coast. All these historical events have been classified as a  
330 magnitude between 1 and 3 in the Tsunami Intensity Scale (on a scale of 6 for a maximum  
331 intensity, Maramai et al., 2014). Since these different historical events have a magnitude equal or  
332 lower than the Boumerdes-Zemmouri tsunami (3 in the Tsunami Intensity Scale), and that this  
333 event did not have affected significantly the La Manga sandbar and the Province of Murcia,  
334 considering the available data, historical tsunami events do not seem to be associated to the  
335 different sand layers in the Mar Menor lagoon for the last 500 years. From the “Catálogo de  
336 Tsunamis en las Costas Españolas”, none tsunamis are recorded along the South Eastern coast of  
337 Spain from -218 BC to 1756 AD. No information on the existence of tsunamis is recorded over  
338 longer periods of time. However, more than 100 boulders were identified along the coastal zone



339 of Algiers and Maouche et al. (2009) suggested that the deposition of the biggest boulders could  
340 be attributed to tsunami events. The radiocarbon results highlight two groups of boulders dated to  
341 around 419 AD and 1700 AD. Although no historical accounts report these events, tsunami  
342 events are extremely rare and of low magnitude and cannot be at the origin of the different sand  
343 layers in the Mar Menor lagoon.

344 To determine which historical events may let sandy layers, we compared our high-resolution  
345 record of past extreme sea events from the core MM2 to the catalogue of historical storm and  
346 tsunami events in the area. The first coarse-grained event layer has been dated at 80 cal. BP (i.e.  
347 1880 A.D+/-30 years). This sandy deposit could be associated to the storm of November first,  
348 1869, recorded in many city archives between Cartagena and Torrevieja and in the Mar Menor,  
349 and considered as the most catastrophic storm event in the Province of Murcia for the last 200  
350 years. In the core MM2, no sand layers are consistent with the Algerian tsunamis dated to around  
351 419 AD and 1700 AD (Figure 8). There is clear evidence that this sand layer is compatible with  
352 large storm waves.

353

### 354 5.3 Storm activity in the context of past climatic changes

355

356 Based on our  $^{14}\text{C}$  age model, marine coarse grained event layers occurred around 5250, 4000,  
357 3600, 3010, 2300, 1350, 650 and 80 years cal B.P. Except one period dated at 3600 years cal  
358 B.P., the seven other periods of most frequent surge events in the Mar Menor lagoon seem to  
359 coincide with the coldest periods in Europe during the late Holocene, taking into account  
360 chronological uncertainty (Figure 8, Bond et al., 2001). A spectral analysis was performed on the  
361 ca. 6.5-kyr time series of the sand percentage from the MM2 sequence. The results show four



362 major frequencies with high spectral power densities and significant F-test values at ca.  $8 \times 10^{-4}$ ,  
363  $1.4 \times 10^{-3}$ ,  $1.8 \times 10^{-3}$ , and  $3.1 \times 10^{-3} \text{ yr}^{-1}$  (Figure 9A). Considering the full width at half maximum  
364 (FWHM) of these peaks on the MTM spectrum, this yields respective periodicities of  $1228 \pm 327$ ,  
365  $732 \pm 80$ ,  $562 \pm 58$ , and  $319 \pm 16 \text{ yr}$  for the MM2 sand % proxy. Multi-centennial to millennial  
366 timescale climate variabilities similar to these periodicities have been reported in the literature for  
367 the Holocene (Bond et al., 1997, 2001; Langdon et al., 2003; Debret et al., 2007, 2009; Wanner et  
368 al., 2011; Kravchinsky et al., 2013; Soon et al., 2014). Amongst the well-known proxies that have  
369 revealed a millennial-scale climate variability during the Holocene, the ice-rafted debris (IRD)  
370 indices in North Atlantic developed by Bond et al. (1997, 2001) present a cyclicity of  $1470 \pm 500$   
371 yr, which matches the  $1228 \pm 327 \text{ yr}$  periodicity evidenced in the Mar Menor lagoon, considering  
372 the respective uncertainties on the periodicities. When filtering the raw data of the Mar Menor  
373 sand % record by a Gaussian filter with a frequency of  $8 \times 10^{-4} \text{ yr}^{-1}$  (1228 years), it appears 6  
374 cycles with a noteworthy enhancement of the cyclic amplitude after 5500 cal yr BP (Figure 9B).  
375 The five ascending phases occurring on the 1228-yr filtered curve at ca. 5715/5115, 4525/3945,  
376 3365/2775, 2145/1215, and 575/-35 cal yr BP approximate the high storm activity periods  
377 evidenced in the French Mediterranean lagoon of Pierre-Blanche for the last 7000 years (Sabatier  
378 et al., 2012).

379 The origin of the storminess periods evidenced by the spectral analysis in the Mar Menor lagoon  
380 can be discussed in the light of previous works mentioning analogous climate variabilities during  
381 the Holocene. Bond et al. (1997, 2001) associated the  $1470 \pm 500 \text{ yr}$  IRD cycle to a solar forcing,  
382 amplified by a change of North Atlantic Deep Water production. Langdon et al. (2003) found a  
383 sub-millennial climate oscillation in Scotland possibly related to the North Atlantic thermohaline  
384 circulation (THC). Moreover, Debret et al. (2007, 2009) showed a cyclicity of 1500 yr since the  
385 Mid-Holocene probably link to an internal forcing due to the THC.



386 Concerning the multi-centennial periodicities, Soon et al. (2014) used global proxies to evidence  
387 a 500-yr fundamental solar mode and to identify intermediary derived cycles at 700 and 300-yr  
388 which could be rectified responses of the Atlantic THC to external solar modulation and pacing.  
389 Kravchinsky et al. (2013) found also a 500-yr climate cycle in the southern Siberia presumed  
390 driven by increased solar insolation and possibly amplified by other mechanisms. Some authors  
391 found a relationship between the ca. 700-yr period and the monsoonal/ITCZ regimes in equatorial  
392 Africa (Russell et al., 2003; Russell and Johnson, 2005), southern Asian (Staubwasser et al.,  
393 2003), and eastern Arabian Sea (Sarkar et al., 2000), while other authors suggested that the ca.  
394 700-800 yr period could be a subharmonic mode derived from the fundamental 1500-year cycle  
395 of the THC (Von Rad et al., 1999; Wang et al., 1999). Besides, Rimbu et al. (2004) mentioned a  
396 700 yr variability from sea-surface temperature (SST) records in the tropical and North Atlantic.  
397 Hence, our results seem to indicate that the Late Holocene multi-centennial variability of the  
398 cyclogenesis in Western Mediterranean was steered by both, external (solar) and internal  
399 (THC/ITCZ) forcings. Further investigations of additional sequences and high-resolution coastal  
400 imagery will be required to assert reliably the origin of these multi-centennial periods in the  
401 Mediterranean area.

402

## 403 7. Conclusion

404 This study provides a 6500-yr high-resolution record of past overwash events using a multi-proxy  
405 approach of a sediment core from the Mar Menor lagoon in Spain in the Western Mediterranean  
406 Sea. Eight sandy layers are preserved in the core and seems to be associated to periods of  
407 increased extreme sea events. The results indicate little likelihood of a tsunami origin for these  
408 coarse grained layers, although historical tsunami events are recorded in this area. These surge



409 events seem to coincide with climatic cold periods in Europe during the late Holocene,  
410 suggesting a control by a climatic mechanism for periods of increased storm activity. From the  
411 available data, we have identified seven periods of high storm activity at around 5250, 4000,  
412 3600, 3010, 2300, 1350, 650 and 80 years cal B.P. Except one period dated at 3600 years cal  
413 B.P., the seven other periods of most frequent surge events in the Mar Menor lagoon seem to  
414 coincide with the coldest periods in Europe during the late Holocene, taking into account  
415 chronological uncertainty. Spectral analyses performed on the sand % revealed four major  
416 periodicities of  $1228 \pm 327$ ,  $732 \pm 80$ ,  $562 \pm 58$ , and  $319 \pm 16$  yr. The origin of the storminess  
417 periods evidenced by the spectral analysis in the Mar Menor lagoon can be discussed in the light  
418 of previous works mentioning analogous climate variabilities during the Holocene. Our results  
419 seem to indicate that the Late Holocene multi-centennial variability of the cyclogenesis in  
420 Western Mediterranean was steered by both, external (solar) and internal (THC/ITCZ) forcings.  
421 However, further investigations, such as additional coring, high-resolution coastal imagery, are  
422 needed to better constrain the main cause of these multiple-events.

423

424

#### 425 Acknowledgments

426

427 The authors would like to thank all participants in the coring expedition, particularly E. Regnier  
428 (Technician, LSCE - IPSL, Paris) for his collaboration in the various stages of this study. This  
429 study is funded by the MISTRALS PALEOMEX project. We thank the Laboratoire de Mesure  
430  $^{14}\text{C}$  (LMC14) ARTEMIS in the CEA Institute at Saclay (French Atomic Energy Commission) for  
431 the  $^{14}\text{C}$  analyses.



432

433

434 **References**

435

436 Álvarez-Gómez, J. A., González, M., and Otero, L.: Tsunami hazard at the Western  
437 Mediterranean Spanish coast from seismic sources, *Natural Hazards and Earth System*  
438 *Science*, 11, 227-240, 2011.

439 Berger, A., Melice, J.-L., Hinnov, L.: A strategy for frequency spectra of Quaternary climate  
440 records. *Climate Dynamics* 5, 227-240, 1991.

441 Bond, G., Kromer, B., Beer, J., Muscheler, R., Evans, M. N., Showers, W., Hoffmann, S., Lotti-  
442 Bond, R., Hajdas, I., and Bonani, G.: Persistent solar influence on North Atlantic climate  
443 during the Holocene, *Science*, 294, 2130-2136, 2001.

444 Bond, G., Showers, W., Cheseby, M., Lotti, R., Almasi, P., DeMenocal, P., Priore, P., Cullen, H.,  
445 Hajdas, I., Bonani, G.: A pervasive millennial-scale cycle in North Atlantic Holocene and  
446 Glacial climates. *Science* 278, 1257-1266, 1997.

447 Bronk Ramsey, C., Development of the Radiocarbon calibration program OxCal, *Radiocarbon*,  
448 43, 355-363, Proceedings of 17th International 14C Conference, 2001.

449 Bronk Ramsey, C., Deposition models for chronological records, *Quaternary Science reviews*,  
450 27, 42-60, 2008.

451 Debret, M., Bout-Roumazelles, V., Grousset, F., Desmet, M., McManus, J.F., Massei, N., Sebag,  
452 D., Petit, J.-R., Copard, Y., Trentesaux, A.: The origin of the 1500-year climate cycles in  
453 Holocene North-Atlantic records. *Climate of the Past* 3, 569-575, 2007.



- 454 Debret, M., Sebag, D., Crosta, X., Massei, N., Petit, J.-R., Chapron, E., Bout-Roumazeilles, V.:  
455 Evidence from wavelet analysis for a mid-Holocene transition in global climate forcing.  
456 Quaternary Science Reviews 28, 2675-2688, 2009.
- 457 Desprat, S., Sanchez-Goni, M.F., Loutre, M.-F.: Revealing climatic variability of the last three  
458 millennia in northwestern Iberia using pollen influx data. Earth and Planetary Science  
459 Letters 213, 63-78, 2003.
- 460 Dezileau, L., Pérez-Ruzafa, A., Camps P., Blanchemanche P., Grafenstein U., Holocene  
461 variations of radiocarbon reservoir ages in the Mar Menor lagoon system, Radiocarbon, in  
462 prep.
- 463 Dezileau, L., Sabatier, P., Blanchemanche, P., Joly, B., Swingedouw, D., Cassou, C., Castaings,  
464 J., Martinez, P., and Von Grafenstein, U.: Intense storm activity during the Little Ice Age  
465 on the French Mediterranean coast, Palaeogeography, Palaeoclimatology, Palaeoecology,  
466 299, 289-297, 2011.
- 467 Dezileau L., Lehu R., Lallemand S., Hsu S-K., Babonneau N., Ratzov G., Lin A.T., Dominguez  
468 S., Historical reconstruction of submarine earthquakes using  $^{210}\text{Pb}$ ,  $^{137}\text{Cs}$  and  $^{241}\text{Am}$   
469 turbidite chronology and radiocarbon reservoir age estimation off East Taiwan.  
470 Radiocarbon. doi:10.1017/RDC.2015.3, 2016.
- 471 Donnelly, J. P., Webb III, T., Murnane, R., and Liu, K.: Backbarrier sedimentary records of  
472 intense hurricane landfalls in the northeastern United States, Hurricanes and Typhoons:  
473 Past, Present, and Future, 58-95, 2004.
- 474 Dubar, M.: Approche climatique de la période romaine dans l'est du Var : recherche et analyse  
475 des composantes périodiques sur un concrétionnement centennal (Ier-IIe siècle apr. J.-C.)  
476 de l'aqueduc de Fréjus. ArchéoSciences 30, 163-171, 2006.



- 477 Engel, M., and Brückner, H.: The identification of palaeo-tsunami deposits—a major challenge in  
478 coastal sedimentary research, *Dynamische Küsten—Grundlagen, Zusammenhänge und*  
479 *Auswirkungen im Spiegel angewandter Küstenforschung*. Proceedings of the 28th Annual  
480 Meeting of the German Working Group on Geography of Oceans and Coasts, 2011, 22-25,  
481 Gaertner, M.A., Jacob, D., Gil, V., Domínguez, M., Padorno, E., Sánchez, E., Castro, M. :  
482 Tropical cyclones over the Mediterranean Sea in climate change simulations. *Geophysical*  
483 *Research Letters* 34. doi:10.1029/2007GL029977, 1-5, 2007.
- 484 Harremoës, P., Topsoe, F.: Maximum entropy fundamentals. *Entropy* 3, 191-226, 2001.
- 485 IGN: Catalogo de Tsunamis en las Costas Espanolas. Instituto Geografico Nacional, [www.ign.es](http://www.ign.es),  
486 2009.
- 487 Jimenez de Gregorio, F.: *El Municipio de San Javier en la historia del Mar Menor y su ribera*.  
488 Ayuntamiento de San Javier, Murcia, 1957.
- 489 Kelletat, D., and Schellmann, G.: Tsunamis on Cyprus: field evidences and 14C dating results,  
490 *Zeitschrift für Geomorphologie*, NF, 19-34, 2002.
- 491 Kjerfve, B.: Coastal lagoons. In Kjerfve B (ed). *Coastal lagoon processes*. Elsevier  
492 Oceanography Series 60: 1-8, 1994.
- 493 Kortekaas, S., and Dawson, A.: Distinguishing tsunami and storm deposits: an example from  
494 Martinhal, SW Portugal, *Sedimentary Geology*, 200, 208-221, 2007.
- 495 Kravchinsky, V.A., Langereis, C.G., Walker, S.D., Dlusskiy, K.G., White, D.: Discovery of  
496 Holocene millennial climate cycles in the Asian continental interior: Has the sun been  
497 governing the continental climate? *Global and Planetary Change* 110, 386-396, 2013.
- 498 Lambeck, K., and Bard, E.: Sea-level change along the French Mediterranean coast for the past  
499 30 000 years, *Earth and Planetary Science Letters*, 175, 203-222, 2000.



- 500 Langdon, P.G., Barber, K.E., Hugues, P.D.M.: A 7500-year peat-based palaeoclimatic  
501 reconstruction and evidence for an 1100-year cyclicality in bog surface wetness from Temple  
502 Hill Moss, Pentland Hills, southeast Scotland. *Quaternary Science Reviews* 22, 259-274,  
503 2003.
- 504 Lionello, P., Bhend, J., Buzzi, A., Della-Marta, P.M., Krichak, S., Jansá, A., Maheras, P., Sanna,  
505 A., Trigo, I.F., Trigo, R. : Cyclones in the Mediterranean region: climatology and effects on  
506 the environment, in *Mediterranean Climate Variability*. In: Lionello, P., Malanotte-Rizzoli,  
507 P., Boscolo, R. (Eds.), *Mediterranean Climate Variability. : Developments in Earth and*  
508 *Environmental Sciences*, 4. Elseviered., 324–372, 2006.
- 509 Maouche, S., Morhange, C., and Meghraoui, M.: Large boulder accumulation on the Algerian  
510 coast evidence tsunami events in the western Mediterranean, *Marine Geology*, 262, 96-104,  
511 2009.
- 512 Maramai, A., Brizuela, B., and Graziani, L.: The Euro-Mediterranean Tsunami Catalogue,  
513 *Annals of Geophysics*, 57, S0435, 2014.
- 514 Morhange, C., Marriner, N., and Pirazzoli, P. A.: Evidence of Late-Holocene Tsunami Events in  
515 Lebanon *Z. Geomorphol NFSuppl.-Bd.*, 146, 81-95, 2006.
- 516 Morton, R. A., Gelfenbaum, G., and Jaffe, B. E.: Physical criteria for distinguishing sandy  
517 tsunami and storm deposits using modern examples, *Sedimentary Geology*, 200, 184-207,  
518 2007.
- 519 Navarro, F.: Observaciones sobre el Mar Menor (Murcia). *Notas y resúmenes del Instituto*  
520 *Español de Oceanografía*, Ser. II, 16:1-63, 1927.



- 521 Paillard, D., Labeyrie, L., Yiou, P.: Macintosh program performs time-series analysis. EOS  
522 Transactions AGU 77(39), 379-379, 1996.
- 523 Pardo-Iguzquiza, E., Rodriguez-Tovar, F.J.: Maximum entropy spectral analysis of climatic time  
524 series revisited: Assessing the statistical significance of estimated spectral peaks. Journal of  
525 Geophysical Research 111, D10102, 2006.
- 526 Percival, D.B., Walden, A.T.: Spectral analysis for physical applications: multitaper and  
527 conventional univariate techniques. Cambridge University Press, New York, 583 p, 1993.
- 528 Pérez-Ruzafa, A., Marcos, C., Pérez-Ruzafa, I., and Ros, J.: Evolución de las características  
529 ambientales y de los poblamientos del Mar Menor (Murcia, SE de España), Anales de  
530 Biología, 1987, 53-65,
- 531 Pérez-Ruzafa, A., Marcos-Diego, C., and Ros, J.: Environmental and biological changes related  
532 to recent human activities in the Mar Menor (SE of Spain), Marine Pollution Bulletin, 23,  
533 747-751, 1991.
- 534 Pérez-Ruzafa, A., Marcos, C., and Gilabert, J.: The ecology of the Mar Menor coastal lagoon: a  
535 fast-changing ecosystem under human pressure, Coastal Lagoons. CRC Press, Boca Racon,  
536 392-421, 2005.
- 537 Pirazzoli, P. A.: World atlas of Holocene sea-level changes, Elsevier Oceanography Series, 58, 1-  
538 280, 1991.
- 539 Raji, O., Dezileau L., Snoussi M., and Niazi, S.: Extreme sea events during the last millennium in  
540 North-East of Morocco. Natural Hazards and Earth System Sciences, 15,203-211, 2015.
- 541 Reimer P.J., McCormac F.G.: Marine radiocarbon reservoir corrections for the Mediterranean  
542 and Aegean seas. Radiocarbon 44(1):159–66, 2002.



- 543 Rimbu, N., Lohmann, G., Lorenz, S.J., Kim, J.H., Schneider, R.R.: Holocene climate variability  
544 as derived from alkenone sea surface temperature and coupled ocean-atmosphere model  
545 experiments. *Climate Dynamics* 23, 215-227, 2004.
- 546 Russell, J.M., Johnson, T.C.: Late Holocene climate change in the North Atlantic and equatorial  
547 Africa: Millennial-scale ITCZ migration. *Geophysical Research Letters* 32, L17705, 2005.
- 548 Russell, J.M., Johnson, T.C., Talbot, M.R.: A 725 yr cycle in the climate of central Africa during  
549 the late Holocene. *Geology* 31(8), 677-680, 2003.
- 550 Sabatier, P., Dezileau, L., Blanchemanche, P., Siani, J., Condomines, M., Bentaleb, I., Piques, G.:  
551 Holocene variations of radiocarbon reservoir ages in a Mediterranean lagoonal system.  
552 *Radiocarbon*, 52, (1), 91-102, 2010.
- 553 Sabatier, P., Dezileau, L., Colin, C., Briquieu, L., Bouchette, F., Martinez, P., Siani, G., Raynal,  
554 O., Von Grafenstein, U.: 7000 years of paleostorm activity in the NW Mediterranean Sea in  
555 response to Holocene climate events. *Quaternary Research* 2012, 1-11, 2012.
- 556 Sarkar, A., Ramesh, R., Somayajulu, B.L.K., Agnihotri, R., Jull, A.J.T., Burr, G.S.: High  
557 resolution Holocene monsoon record from the eastern Arabian Sea. *Earth and Planetary  
558 Science Letters* 177, 209-218, 2000.
- 559 Scileppi, E., Donnelly, J.P. : Sedimentary evidence of hurricane strikes in western Long Island,  
560 NY. *Geochemistry, Geophysics and Geosystems* 8, Q06011. doi:10.1029/2006GC001463,  
561 2007.
- 562 Seisdedos, J., Mulas, J., González de Vallejo, L. I., Rodríguez Franco, J. A., Gracia, F. J., Del  
563 Río, L., y Garrote, J. :Estudio y cartografía de los peligros naturales costeros de la región  
564 de Murcia. *Boletín Geológico y Minero*, 124 (3): 505-520, 2013.



- 565 Siani G., Paterne M., Michel E., Sulpizio R., Sbrana A., Arnold M., Haddad G. : Mediterranean  
566 sea surface radiocarbon age changes since the last glacial maximum. *Science*  
567 294(5548):1917–20, 2001.
- 568 Soon, W., Velasco Herrera, V.M., Selvaraj, K., Traversi, R., Usoskin, I., Arthur Chen, C.-T.,  
569 Lou, J.-Y., Kao, S.-J., Carter, R.M., Pipin, V., Severi, M., Becagli, S.: A review of  
570 Holocene solar-linked climatic variation on centennial to millennial timescales: Physical  
571 processes, interpretative frameworks and a new multiple cross-wavelet transform  
572 algorithm. *Earth-Science Reviews* 134, 1-15, 2014.
- 573 Staubwasser, M., Sirocko, F., Grootes, P.M., Segl, M.: Climate change at the 4.2 ka BP  
574 termination of the Indus valley civilization and Holocene south Asian monsoon variability.  
575 *Geophysical Research Letters* 30(8), 1425, 2003.
- 576 Thomson, D.J.: Spectrum estimation and harmonic analysis. *Proceedings of the IEEE* 70(9),  
577 1055-1096, 1982.
- 578 Thomson, D.J.: Time series analysis of Holocene climate data. *Philosophical Transactions of the*  
579 *Royal Society of London, Series A, Mathematical and Physical Sciences* 330, 601-616,  
580 1990.
- 581 Trigo, I.F., Davies, T.D., Bigg, G.R., : Decline in Mediterranean rainfall caused by weakening of  
582 Mediterranean cyclones. *Geophysical Research Letters* 27, 2913–2916, 2000.
- 583 Von Rad, U., Schaaf, M., Michels, K.H., Schulz, H., Berger, W.H., Sirocko, F. A 5000-yr Record  
584 of Climate Change in Varved Sediments from the Oxygen Minimum Zone off Pakistan,  
585 Northeastern Arabian Sea. *Quaternary Research* 51, 39-53, 1999.
- 586 Wang, L., Sarnthein, M., Erlenkeuser, H., Grimalt, J., Grootes, P., Heilig, S., Ivanova, E.,  
587 Kienast, M., Pelejero, C., Pflaumann, U.: East Asian monsoon climate during the Late

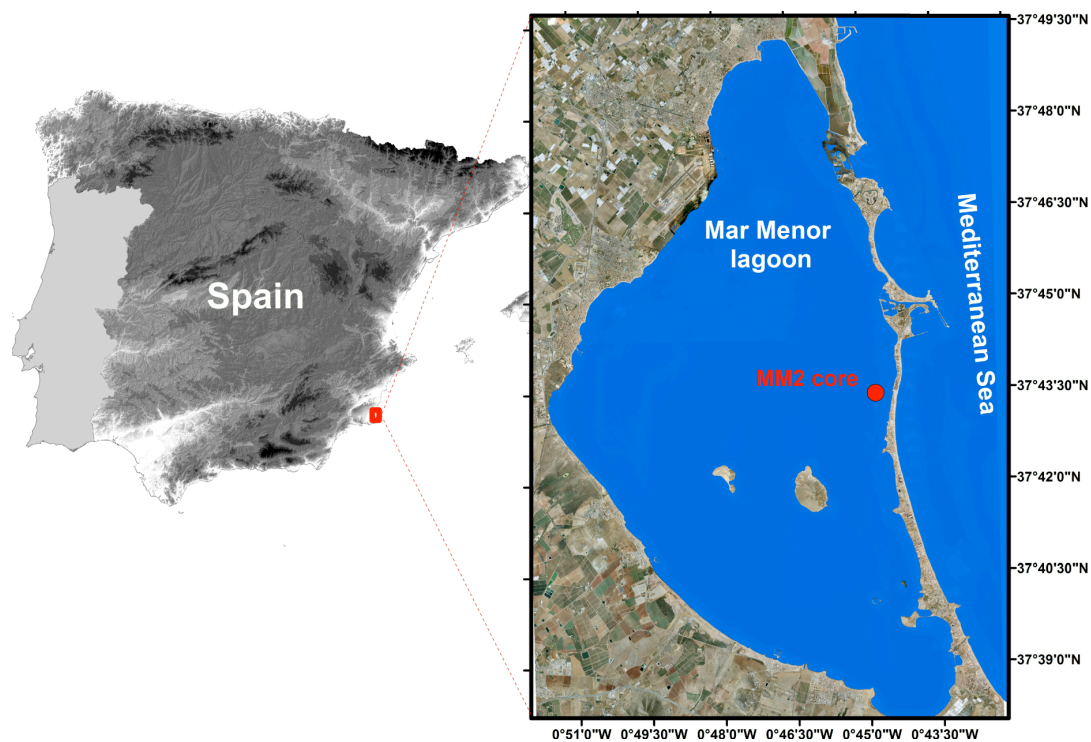


- 588 Pleistocene: high-resolution sediment records from the South China Sea. *Marine Geology*  
589 156, 245-284, 1999.
- 590 Wang, X., Liu, P.L.-F.,: A numerical investigation of Boumerdes-Zemmouri (Algeria)  
591 earthquake and tsunامي. *Computer Modeling in Engineering Science* 10 (2), 171–184,  
592 2005.
- 593 Wanner, H., Solominac, O., Grosjean, M., Ritz, S.P., Jetel, M.: Structure and origin of Holocene  
594 cold events. *Quaternary Science Reviews* 30, 3109-3123, 2011.
- 595 Zoppi U., Albani A., Ammerman A.J., Hua Q., Lawson E.M., Serandrei Barbero R. :Preliminary  
596 estimate of the reservoir age in the Lagoon of Venice. *Radiocarbon* 43(2A):489–94, 2001.  
597  
598  
599



600 *Figures captions*

601  
602  
603  
604  
605  
606  
607  
608  
609  
610



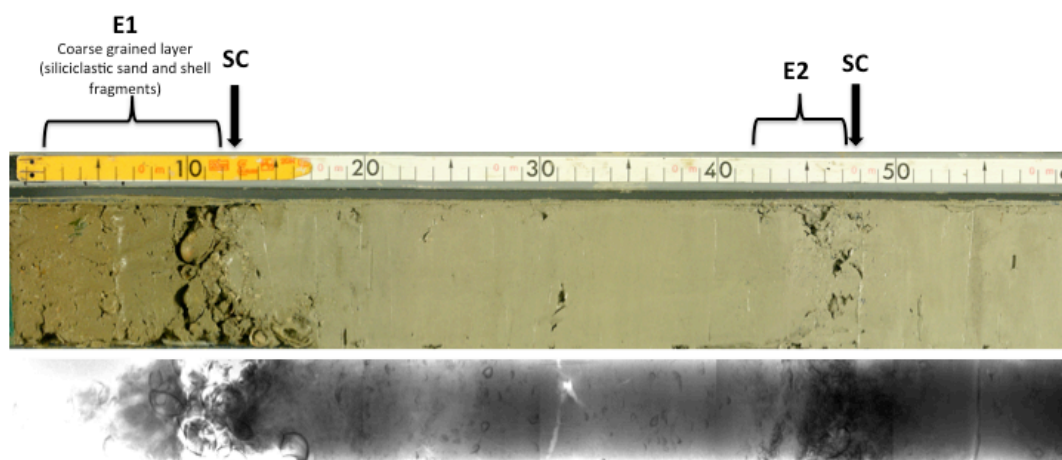
615  
616  
617  
618  
619  
620  
621  
622  
623  
624  
625  
626  
627  
628  
629  
  
630  
  
631  
  
632  
  
633

**Figure 1.** Map of the Mar Menor lagoon with localisation of the core MM2.



634

635



636

637

638

639 **Figure 2.** Photography and X-ray of the core MM2 (0 and 60 cm). Coarse grained layers are a  
640 mixture of siliciclastic sand and shell fragments. These layers have often sharp contacts (SC)  
641 with the clay and silt sediments below.

642

643

644

645

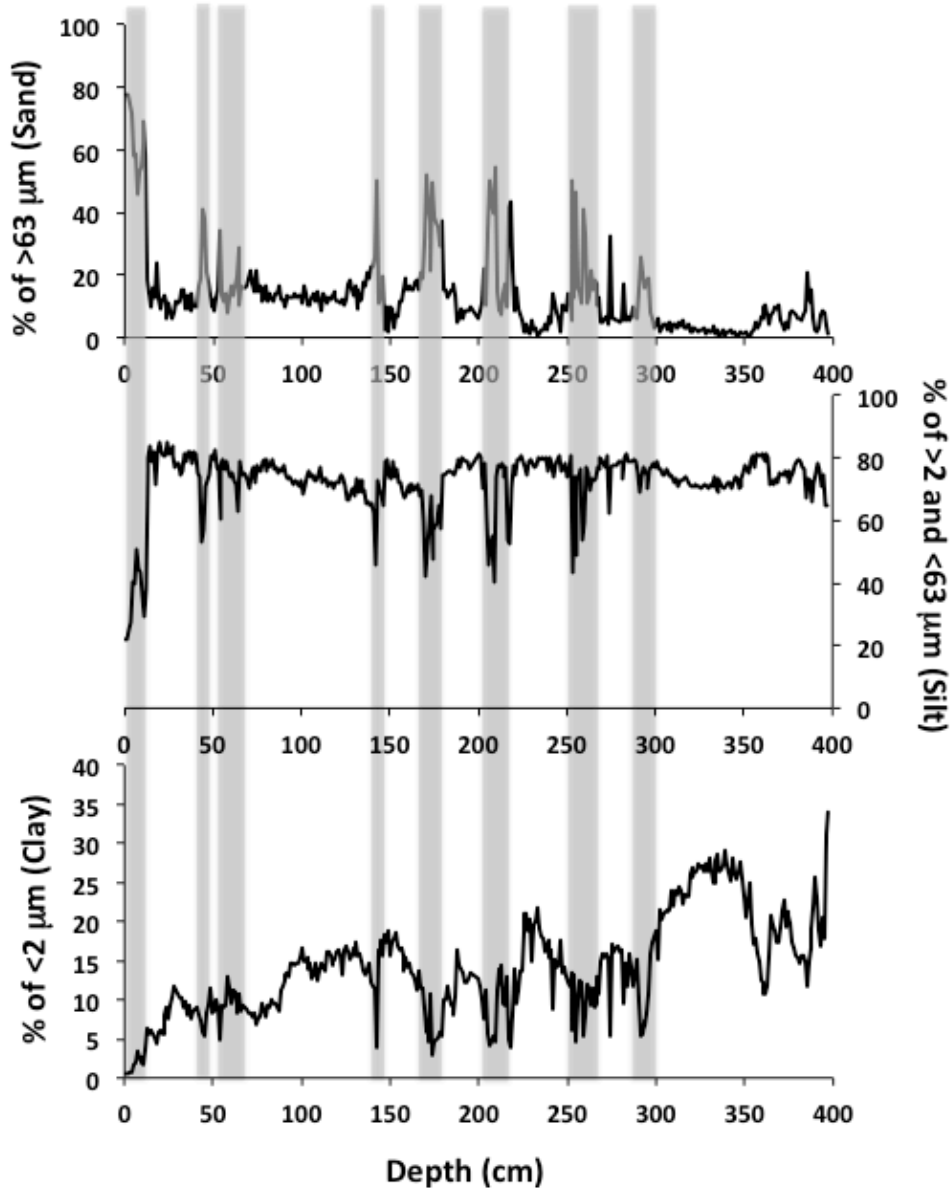
646

647

648

649

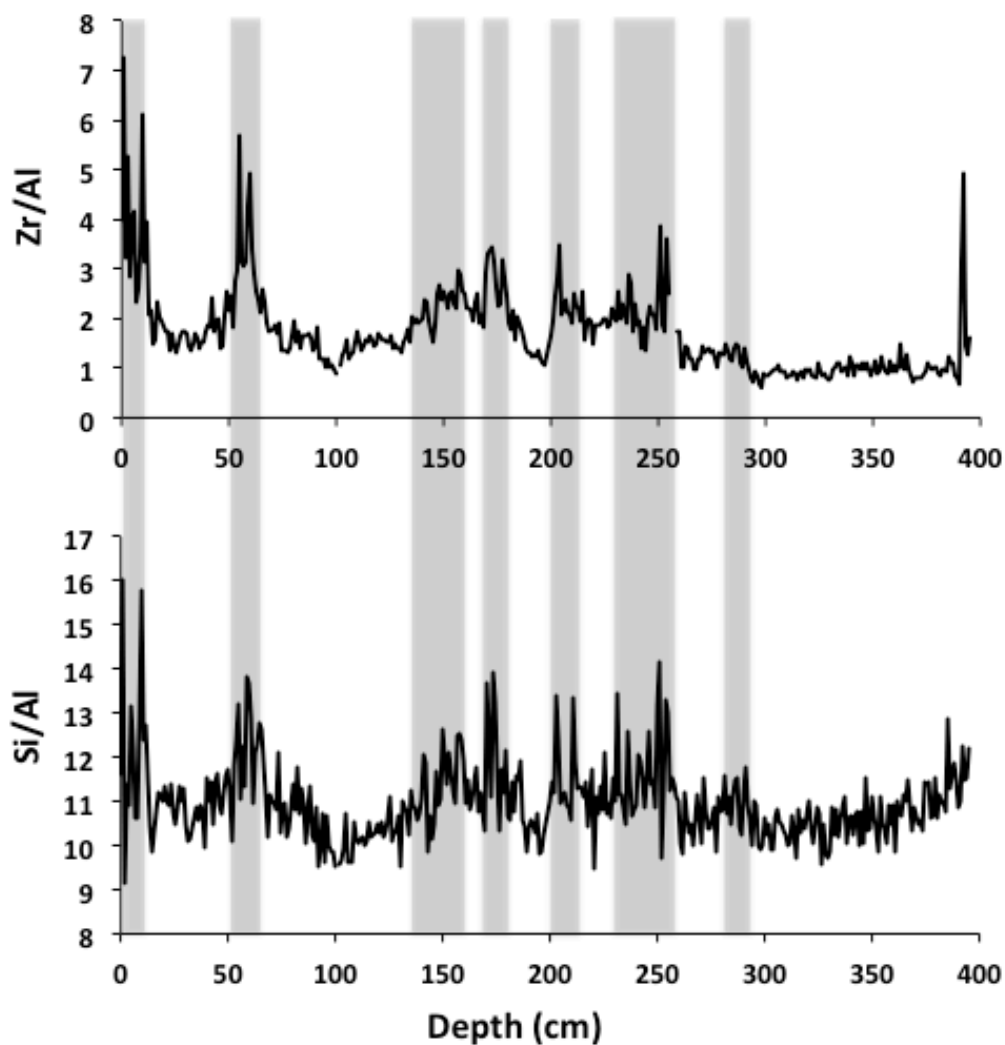
650



651

652 **Figure 3.** Grain size population from the Mar Menor MM2 record with clay (<2 μm), silt (>2 and  
653 <63 μm) and sand fraction (>63μm). Shaded areas mark the main variations of the sand fraction.

654



655

656

657

658 **Figure 4.** XRF records from the core MM2 with down-core variations of ratio Zr/Al and Si/Al.

659 Shaded areas mark the main variations of Zr/Al and Si/Al.

660

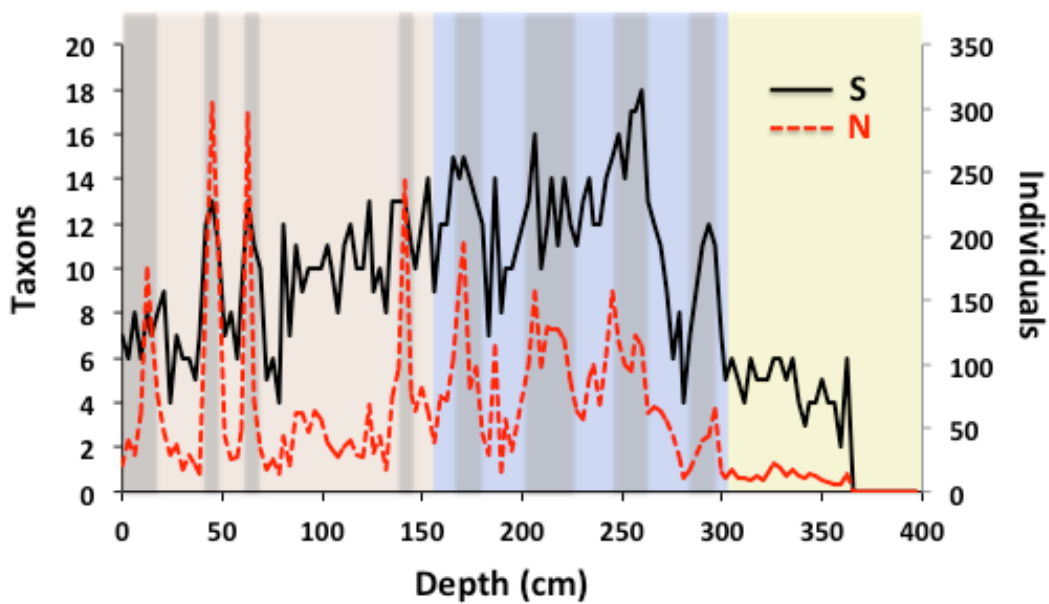
661



662

663

664



665

666 **Figure 5.** Taxon and specie richness with depth from the core MM2.

667

668

669

670

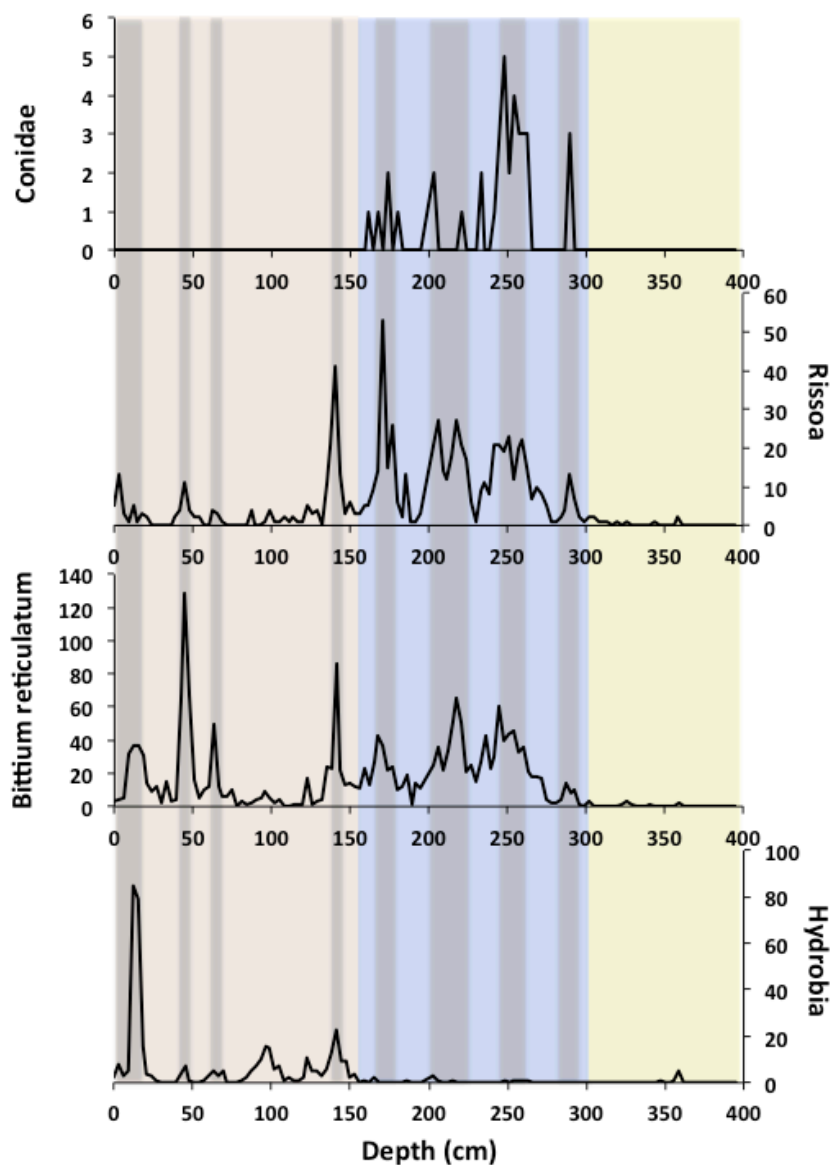
671

672

673

674

675



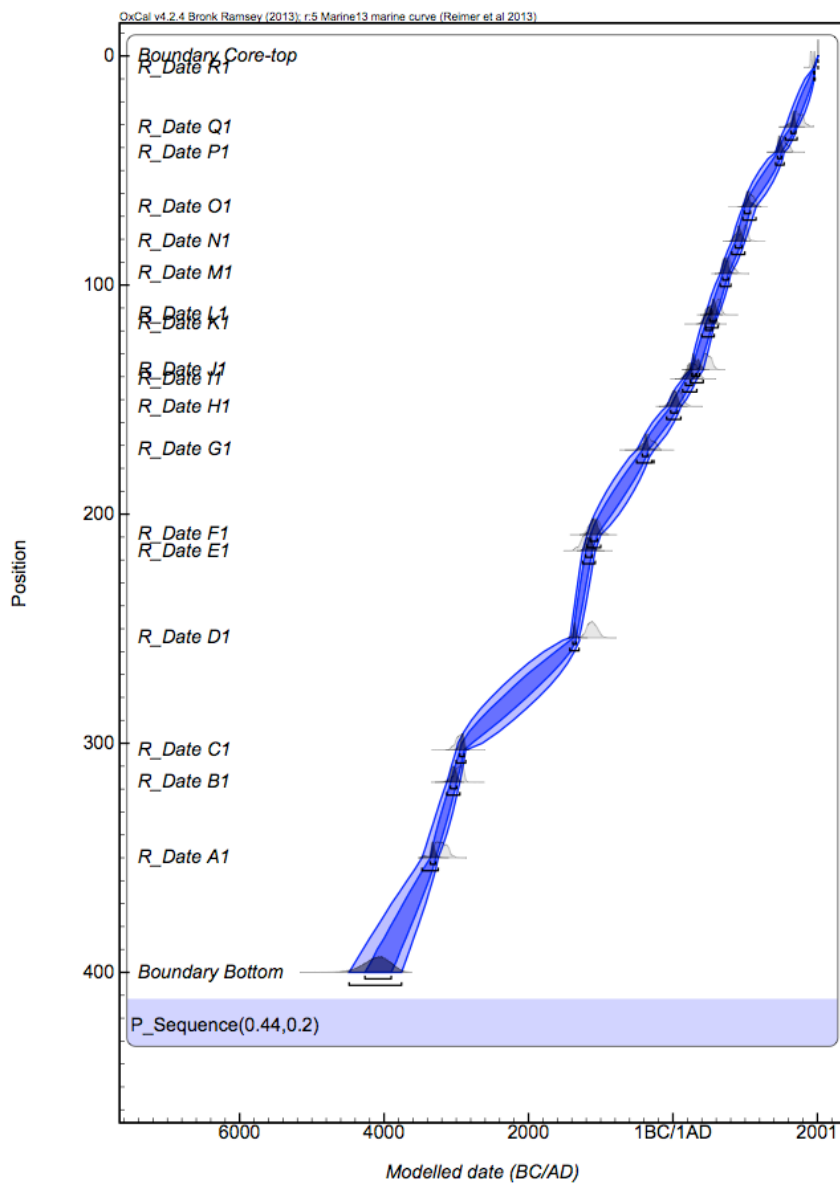
676

677 **Figure 6.** Evolution in mollusc population with depth: lagoonal specie (*Hydrobia acuta*); typical  
678 marine specie (*Conus ventricosus*: Conidae), marine influence (*Bittium Reticulatum* and *Pusillina*  
679 *lineolata*: Rissoa).

680



681

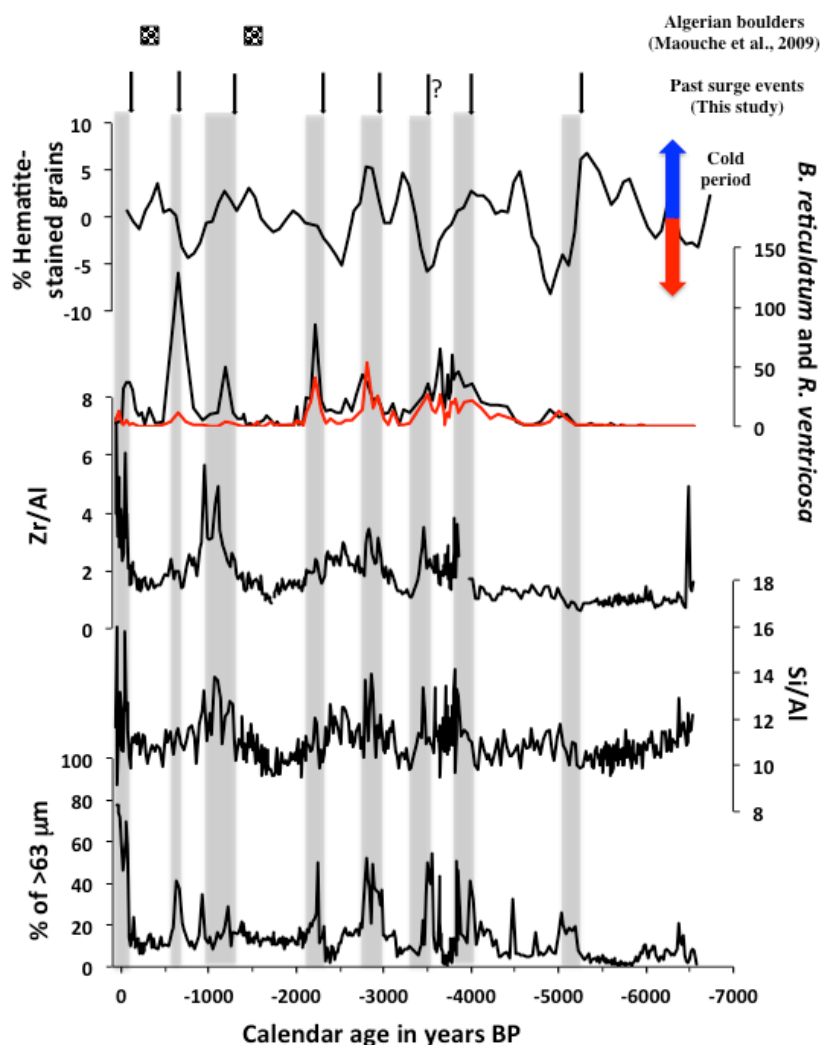


682

683 **Figure 7.** Age vs Depth for the core MM2. The Age model was calculated using OxCal 4 with 17

684 <sup>14</sup>C dates.

685



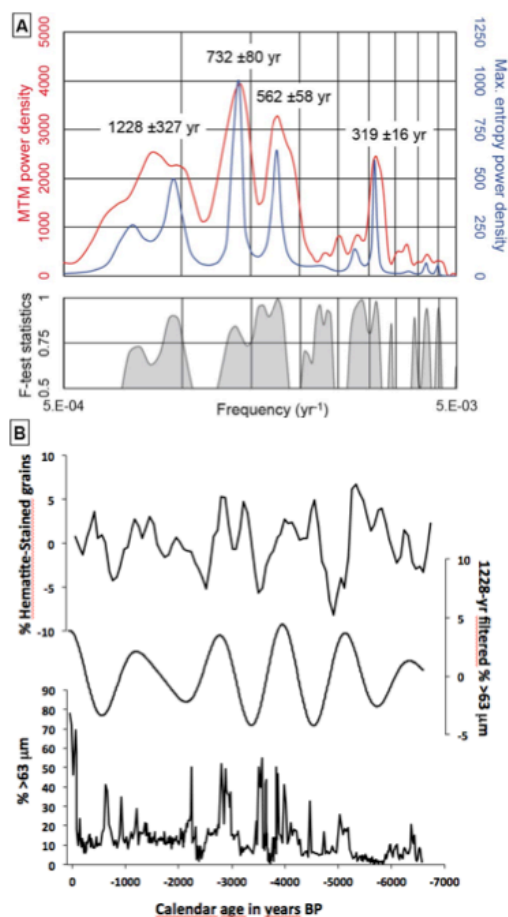
686

687

688 **Figure 8.** Core MM2 with from bottom to top: Grain size (sand fraction); Si/Al and Zr/Al XRF  
689 ratio; number of *B. reticulatum* and *R. Ventricosa*, % Hematite-stained grains (Bond et al., 1997,  
690 2001), ages of Algerian boulders (Maouche et al., 2009). Grey bands are the past surge events.

691

692



693

694 **Figure 9.** Time series analysis from the Mar Menor MM2 record. (A) Spectral analyses of the %  
695 of sand with AnalySeries v.2.0.8 (Paillard et al., 1996) by using the Multi-Taper method (linear  
696 trend removed, width.ndata product: 1.3; number of windows: 2) and the Maximum entropy  
697 method (linear trend removed, % of series: 40, number of lags: 133). (B) Comparison between  
698 the % Hematite-stained grains (Bond et al., 1997, 2001), the Gaussian filter on the % of sand for  
699 the 1228-yr period (frequency: 0.0008, bandwidth: 0.0002) and the sand fraction of the core  
700 MM2.

701